Theoretical Study of Platinum(0)-Catalyzed Hydrosilylation of Ethylene. Chalk−Harrod Mechanism or Modified Chalk−Harrod Mechanism

Shigeyoshi Sakaki,* Nobuteru Mizoe, and Manabu Sugimoto

Department of Applied Chemistry and Biochemistry, Faculty of Engineering, Kumamoto University, Kurokami, Kumamoto 860-8555, Japan

Received March 16, 1998

A detailed theoretical investigation was performed on all of the transition states and intermediates involved in the Si−H oxidative addition of H−SiR_3 (R = H, Cl, or Me) to Pt-$(PH_3)_2$, ethylene insertion into Pt−H and Pt−SiR_3 bonds, isomerization of the ethylene insertion product, and Si−C and C−H reductive eliminations. In a Chalk−Harrod mechanism, the rate-determining step is the isomerization of Pt$(SiR_3)(C_2H_5)(PH_3)$ formed by ethylene insertion into the Pt−H bond and its activation barrier is 22 kcal/mol for R = H, 23 kcal/mol for R = Me, and 26 kcal/mol for R = Cl (MP4SDQ values are given hereafter). In a modified Chalk−Harrod mechanism, the rate-determining step is the ethylene insertion into the Pt−SiH_3 bond and its barrier is 44 kcal/mol for R = H and Me and 60 kcal/mol for R = Cl. Thus, it should be reasonably concluded that platinum(0)-catalyzed hydrosilylation of ethylene proceeds through a Chalk−Harrod mechanism. Chlorine substituent on Si causes significant and interesting effects on the reaction, since the Pt−$SiCl_3$ bond is much stronger than Pt−SiH_3 and Pt−$SiMe_3$ bonds. A methyl substituent influences the activation barrier of Si−H oxidative addition, ethylene insertion, and Si−C reductive elimination little. Detailed analysis is presented to clarify the reason that ethylene is inserted into the Pt−SiR_3 bond with much more difficulty than into the Pt−H bond, since a modified Chalk−Harrod mechanism is difficult due to the high activation barrier of the ethylene insertion into the Pt−SiR_3 bond. The Si−C reductive elimination was also investigated in detail, since this is a candidate for the rate-determining step of a Chalk−Harrod mechanism. The present calculations indicate that the Si−C reductive elimination occurs more easily in Pt-$(SiR_3)(CH_3)(PH_3)(C_2H_4)$ than in Pt$(SiR_3)(CH_3)(PH_3)_2$, which agrees well with the experimental finding of Ozawa et al. (*J. Am. Chem. Soc.* **1995**, *117*, 8873). The reason is clearly interpreted in terms of a π-back-bonding interaction between Pt d and C_2H_4 π^* orbitals. The ethylene coordination to Pt significantly accelerates the Si−C reductive elimination, and as a result, the Si−C reductive elimination can be clearly excluded from the rate-determining step in a Chalk−Harrod mechanism.

Introduction

Hydrosilylation of alkene, alkyne, and similar compounds is important in synthetic reactions, since organosilicon compounds are useful as an intermediate in organic synthesis.[1] In this regard, the hydrosilylation has been widely investigated and many efforts have been made to clarify the reaction mechanism. One of the important catalysts for hydrosilylation is chloroplatinic acid in alcohol (Speier's catalysts),[2] and Chalk and Harrod proposed the reaction mechanism of platinum-catalyzed hydrosilylation of alkene, which consists of Si−H oxidative addition to metal and alkene insertion into the metal−hydride bond followed by Si−C reductive elimination,[1b−d,3] as shown in Scheme 1.

Then, a modified Chalk−Harrod mechanism was proposed[1b−d,4−6] to explain the formation of vinylsilane, which involves the ethylene insertion into the metal−silyl bond followed by the C−H reductive elimination.

Detailed knowledge on the reaction mechanism, the rate-determining step, intermediates, and transition states is necessary to understand the mechanism well

(1) For instance, see: (a) Speier, J. L. *Adv. Organomet. Chem.* **1979**, *17*, 407. (b) Harrod, J. F.; Chalk, A. J. In *Organic Synthesis via Metal Carbonyls*; Wender, I., Pino, P., Eds.; John Wiley & Sons Ltd.: New York, 1977; Vol. 2, p 673. (c) Tilley, T. D. In *The Chemistry of Organic Silicon Compounds*; Patai, S., Rappoport, Z., Eds.; John Wiley & Sons Ltd.: New York, 1989; p 1415. (d) Ojima, I. In *The Chemistry of Organic Silicon Compounds*; Patai, S., Rappoport, Z., Eds.; John Wiley & Sons Ltd.: New York, 1989; p 1479. (e) Ohsima, K. In *Advances in Metal-Organic Chemistry*; Liebeskind, L. S., Ed.; JAI Press Ltd.: London, 1991; Vol. 2, p 101. (f) Uozumi, Y.; Kitayama, K.; Hayashi, T.; Yanagi, K.; Fukuyo, E. *Bull. Chem. Soc. Jpn.* **1995**, *68*, 713 and references therein.

(2) (a) Speier, J. L.; Webster, J. A.; Barnes, G. H. *J. Am. Chem. Soc.* **1957**, *79*, 974. (b) Saam, J. C.; Speier, J. L. *J. Am. Chem. Soc.* **1958**, *80*, 4104. (c) Ryan, J. W.; Speier, J. L. *J. Am. Chem. Soc.* **1964**, *86*, 895.

(3) Chalk, A. J.; Harrod, J. F. *J. Am. Chem. Soc.* **1965**, *87*, 16.

(4) (a) Schroeder, M. A.; Wrighton, M. S. *J. Organomet. Chem.* **1977**, *128*, 345. (b) Reichel, C. L.; Wrighton, M. S. *Inorg. Chem.* **1980**, *19*, 3858. (c) Randolph, C. L.; Wrighton, M. S. *J. Am. Chem. Soc.* **1986**, *108*, 3366.

(5) (a) Milan, A.; Towns, E.; Maitlis, P. M. *J. Chem. Soc., Chem. Coomun.* **1981**, 673. (b) Milan, A.; Fernandez, M.-J.; Bentz, P.; Maitlis, P. M. *J. Mol. Catal.* **1984**, *26*, 89.

(6) Ojima, I.; Yatabe, M.; Fuchikami, T. *J. Organomet. Chem.* **1984**, *260*, 335.

S0276-7333(98)00190-3 CCC: $15.00
Publication on Web 05/20/1998

Scheme 1

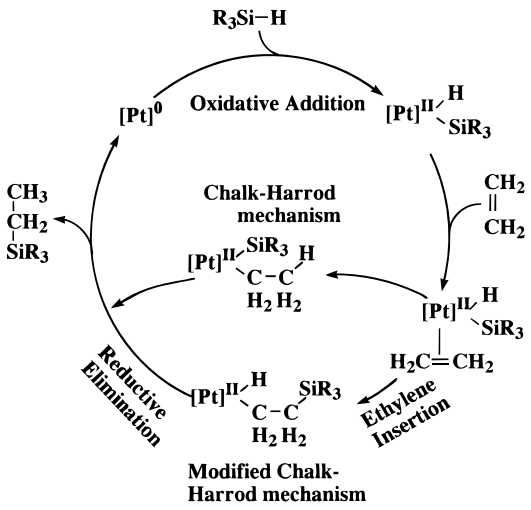

and to further develop this kind of catalytic reaction. To obtain this information, not only experimental work but also theoretical work is useful. In our previous theoretical work, we found that ethylene is more easily inserted into the Pt−H bond than into the Pt−SiH_3 bond.[7] However, this finding is not enough to conclude that a Chalk−Harrod mechanism is more favorable than a modified Chalk−Harrod mechanism; for instance, if the Si−C reductive elimination which occurs as the final step of a Chalk−Harrod mechanism required a higher activation energy than the ethylene insertion into the Pt−SiR_3 bond, then the modified Chalk−Harrod mechanism was more favorable than the Chalk−Harrod mechanism. Thus, we need to investigate the energy change along whole catalytic cycle. Although several variants in the reaction mechanism have been proposed recently for rhodium,[8,9] iridium,[10,11] zirconium,[12] and samarium,[13] it seems reasonable that in the first theoretical study our attention should be focused on a Chalk−Harrod mechanism and a modified Chalk−Harrod mechanism.

In this theoretical work, we investigated platinum(0)-catalyzed hydrosilylation of ethylene with ab initio MO/MP4SDQ, SD-CI, and CCD (coupled cluster with double substitution) methods. Here we adopted a platinum phosphine complex as a model of the catalysts, considering the following reasons: (1) although Speier's catalyst is well-known, Speier's catalyst is considered to be complicated[1b] and its active species is still ambiguous, (2) platinum phosphine complexes have been used as a catalyst for hydrosilylation of alkene and alkyne,[14−16] (3) several model reactions such as the Si−H oxidative addition,[17] alkyne and alkene insertions into a Pt−SiR_3 bond,[18] the Si−C reductive elimination,[19] and Si−C oxidative addition[20−22] have been investigated with platinum phosphine complexes, and (4) interesting asymmetric hydrosilylation of alkene was carried out with platinum phosphine[14b] and similar palladium phosphine complexes.[1f] Our intention with this work is to theoretically estimate the energy change along the whole catalytic cycle of Chalk−Harrod and modified Chalk−Harrod mechanisms. Our purposes here are to (1) clarify through which mechanism the reaction proceeds, (2) demonstrate what elementary step is the rate-determining step, and (3) investigate how much and why the substituents on Si influence the reaction.

Computational Details

The geometries of the reactants, transition states, and products were optimized at the MP2 level for oxidative addition and reductive elimination, since the transition-state structures of these reactions shift somewhat upon introducing electron correlation effects.[23] In the ethylene insertion reaction, however, geometry optimization was performed at the Hartree−Fock (HF) level, since its transition-state structure changes little upon introducing electron correlation effects.[7] The geometry of PH_3 was taken from the experimental structure of the free PH_3 molecule.[24]

MP4SDQ, SD-CI, and CCD calculations were carried out with the optimized geometries to estimate energy changes along the reaction. In SD-CI calculations, the contribution of higher-order excitations was evaluated, according to Davidson−Silver[25] and Pople et al.[26] In CCD calculations, the contribution of single and triple excitations was estimated through fourth-order perturbation using the CCD wave function.[27] The method with this correction is named CCD(ST4) in this work.

In all of the basis set systems employed here, the core electrons of Pt (up to 4f),[28] P, and Cl (up to 2p)[29] were replaced with the effective core potentials (ECPs) of Hay and Wadt. In the smaller basis set system (BS-I), the valence electrons of Pt and P were represented with the (311/311/21)[28] and (21/21)[29] sets, respectively. For Si, C, and H atoms, MIDI-3[30] and (31)[31] sets were employed, respectively. A d polarization

(7) Sakaki, S.; Ogawa, M.; Musashi, Y.; Arai, T. *J. Am. Chem. Soc.* **1994**, *116*, 7258.
(8) Duckett, S. B.; Perutz, R. N. *Organometallics* **1992**, *11*, 90.
(9) Esteruelas, M. A.; Herrero, J.; Oro, L. A. *Organometallics* **1993**, *12*, 2377.
(10) (a) Hostetler, M. J.; Bergman, R. *J. Am. Chem. Soc.* **1990**, *112*, 8621. (b) Hostetler, M. J.; Butts, M. D.; Bergman, R. *Organometallics* **1993**, *12*, 65.
(11) Esteruelas, M. A.; Olivan, M.; Oro, L. A. *Organometallics* **1996**, *15*, 814.
(12) Takahashi, T.; Hasegawa, M.; Suzuki, N.; Saburi, M.; Rousset, C. J.; Fanwick, P. E.; Negishi, E. *J. Am. Chem. Soc.* **1991**, *113*, 8564.
(13) Fu, P. F.; Brard, L.; Li, Y.; Marks, T. J. *J. Am. Chem. Soc.* **1995**, *117*, 7157.
(14) (a) Yamamoto, K.; Hayashi, T.; Kumada, M. *J. Organomet. Chem.* **1971**, *28*, C37. (b) Yamamoto, K.; Hayashi, T.; Kumada, M. *J. Am. Chem. Soc.* **1971**, *93*, 5301.
(15) (a) Green, M.; Spencer, J. L.; Tsipis, C. A. *J. Chem. Soc., Dalton Trans.* **1977**, 1519; **1977**, 1525. (b) Tsipis, C. A. *J. Organomet. Chem.* **1980**, *187*, 427. (c) Tsipis, C. A. *J. Organomet. Chem.* **1980**, *188*, 53.
(16) Prignato, A. L.; Trogler, W. C. *J. Am. Chem. Soc.* **1987**, *109*, 3586.
(17) Shimada, S.; Tanaka, M.; Honda, K. *J. Am. Chem. Soc.* **1995**, *117*, 8289.
(18) Yamashita, H.; Tanaka, M.; Goto, M. *Organometallics* **1993**, *12*, 988; *Organometallics* **1997**, *16*, 4696.
(19) Ozawa, F.; Hikida, T.; Hayashi, T. *J. Am. Chem. Soc.* **1994**, *116*, 2844.
(20) Ciriano, M.; Howard, J. A. K.; Spencer, J. L.; Stone, F. G. A.; Wadepohl, H. *J. Chem. Soc., Dalton Trans.* **1979**, 1749.
(21) Hofmann, P.; Heiss, H.; Neitler, P.; Muller, G.; Lachmann, J. *Angew. Chem., Int. Ed. Engl.* **1990**, *29*, 880.
(22) Yamashita, H.; Tanaka, M.; Honda, K. *J. Am. Chem. Soc.* **1995**, *117*, 8873.
(23) Sakaki, S.; Ogawa, W.; Kinoshita, M. *J. Phys. Chem.* **1995**, *99*, 9933.
(24) Herzberg, G. *Molecular Spectra and Molecular Structure*; D. Von Nostrand Co. Inc.: Princeton, NJ, 1967; Vol. 3, p 610.
(25) Davidson, E. R.; Silver, D. W. *Chem. Phys. Lett.* **1977**, *52*, 403.
(26) Pople, J. A.; Seeger, R.; Krishnan, R. *Int. J. Quantum Chem. Symp.* **1977**, *11*, 149.
(27) Raghavachari, K. *J. Chem. Phys.* **1985**, *82*, 4607.
(28) Hay, P. J.; Wadt, W. R. *J. Chem. Phys.* **1985**, *82*, 299.
(29) Wadt, W. R.; Hay, P. J. *J. Chem. Phys.* **1985**, *82*, 284.
(30) Huzinaga, S.; Andzelm, J.; Klobukowski, M.; Radzio-Andzelm, E.; Sakai, Y.; Tatewaki, H. *Gaussian basis sets for molecular calculations*; Elsevier: Amsterdam, 1984.
(31) Dunning, T. H.; Hay, P. J. In *Methods of Electronic Structure Theory*; Schaeffer, H. F., Ed.; Plenum: New York, 1977; p 1.

function[32] and a p polarization function[31] were added to Si and an active H atom, respectively, where the active H atom is the hydride ligand. This BS-I system was used for geometry optimization. In the larger basis set system (BS-II), the valence electrons of Pt and P were represented with slightly more flexible (311/311/111)[28] and (21/21/1)[29,30] basis sets, respectively, while those of Cl were represented with the same basis set as that in BS−I. Huzinage−Dunning (531111/4211/1) and (721/41/1) basis sets were employed for Si and C, respectively.[31] A p polarization function[31] was added to H, except for the H of PH_3. This BS−II system was used for estimation of the energy change. Gaussian92 and −94 programs[33] were employed for these calculations.

Results and Discussion

In both Chalk−Harrod and modified Chalk−Harrod mechanisms, the Si−H oxidative addition to platinum(0) is involved as a common process. Then, ethylene is inserted into either the Pt−H or Pt−silyl bond, and finally, either the Si−C or C−H reductive elimination occurs to complete the catalytic cycle. We investigated these processes in order.

Si−H Oxidative Addition of H−SiR_3 to $Pt(PH_3)_2$. Since Prignato and Trogler experimentally suggested that Si−H oxidative addition occurs not to a platinum(0) alkene complex but to a platinum(0) bis(phosphine) complex,[16] the oxidative addition of silane to $Pt(PH_3)_2$ was examined here. We omitted a detailed discussion of the geometry change and energy change because this reaction was theoretically investigated in our previous works.[23,24] We will mention only a few of the important points concerning computational levels and substituent effects. As shown in Table 1, the activation energy and the reaction energy slightly fluctuate around the MP2 and MP3 levels but they change little upon going to the CCD(ST4) level from the MP4SDQ level. From these results, it is reasonably suggested that the MP4SDQ method is useful to estimate energy changes.

The reaction energy significantly depends on the substituent on Si; the exothermicity is the greatest in the reaction of H−$SiCl_3$ and the least in the reaction of H−$SiMe_3$. Since the reaction energy can be related to Pt−SiR_3 and H−SiR_3 bond energies, these bond energies were estimated by considering eqs 1−4. First, the Pt−H bond energy was estimated from eqs 1 and 2, then the sum of the Pt−H and Pt−SiR_3 bond energies was evaluated by using eqs 3 and 4, and finally, the Pt−SiR_3 bond energy was calculated by subtracting the Pt−H bond energy from the sum. The H−SiR_3 bond energy was also estimated with eq 4. They are listed in Table 2. The Pt−SiR_3 bond energy can be evaluated in a different way with eqs 5 and 6 However, this estimation was not adopted here since *cis*-$Pt(SiMe_3)_2(PH_3)_2$ is too large to carry out the MP4SDQ calculation. In our previous work,[23] the Pt−H bond energy was calculated with eqs 7 and 8 and compared with the Pt−H bond energy calculated with eqs 1 and 2. The difference between the two estimations is very small. Thus, the Pt−SiR_3 bond energy estimated from eqs 1−4 seems reliable for semiquantitative discussion. Actually, the calculated Pt(II)−$SiMe_3$ bond energy is similar to the experimentally estimated Pt(IV)−$SiMe_3$ bond energy (233 ± 14 kJ/mol), while the Pt oxidation state and the coexisting ligand are different between the present calculation and the experiment.[35,36]

As shown in Table 2, the Pt−$SiCl_3$ bond is the strongest, which clearly suggests that the electron-

$$Pt(PH_3)_2 + H-H \rightarrow cis\text{-}PtH_2(PH_3)_2 \quad (1)$$

$$H-H \rightarrow 2^{\bullet}H \quad (2)$$

$$Pt(PH_3)_2 + H-SiR_3 \rightarrow cis\text{-}PtH(SiR_3)(PH_3)_2 \quad (3)$$

$$H-SiR_3 \rightarrow {}^{\bullet}H + {}^{\bullet}SiR_3 \quad (4)$$

Table 1. Activation Energy (E_a)[a] and Reaction Energy (ΔE)[b]) (kcal/mol)

	E_a	ΔE
	R = H	
HF	8.3	−6.4
MP2	2.0	−24.2
MP3	4.3	−21.7
MP4DQ	0.6	−21.9
MP4SDQ	2.4	−21.9
SD-CI(DS)	1.2	−22.7
SD-CI(P)	0.9	−21.1
CCD(ST4)	2.8	−21.7
	R = Cl	
HF	9.7	−20.3
MP2	1.8	−34.4
MP3	4.8	−33.3
MP4DQ	3.9	−32.7
MP4SDQ	2.8	−32.3
	R = Me	
HF	6.8	2.2
MP2	2.8	−19.9
MP3	4.1	−16.5
MP4DQ	3.5	−16.6
MP4SDQ	3.0	−16.8

[a] E_a= energy difference between the precursor complex and the transition state. [b] ΔE = energy difference between the product and the sum of the reactants (a negative value represents the exothermicity).

$$Pt(PH_3)_2 + R_3Si-SiR_3 \rightarrow cis\text{-}Pt(SiR_3)_2(PH_3)_2 \quad (5)$$

$$R_3Si-SiR_3 \rightarrow 2^{\bullet}SiR_3 \quad (6)$$

$$Pt(PH_3)_2 + H-SiH_3 \rightarrow cis\text{-}PtH(SiH_3)(PH_3)_2 \quad (7)$$

$$H-SiH_3 \rightarrow H^{\bullet} + {}^{\bullet}SiH_3 \quad (8)$$

(32) Sakai, Y.; Tatewaki, H.; Huzinaga, S. *J. Comput. Chem.* **1981**, *2*, 108.

(33) (a) Frisch, A. M. J.; Trucks, G. W.; Head-Gordon, M.; Gill, P. M. W.; Wong, M. W.; Foresman, J. B.; Johnson, B. G.; Schlegel, H. B.; Robb, M. A.; Replogle, E. S.; Gomperts, R.; Andres, J. L.; Raghavachari, K.; Bankley, J. S.; Gonzalez, C.; Martin, R. L.; Fox, D. J.; DeFrees, D. J.; Baker, J.; Stewart, J. J. P.; Pople, J. A. *Gaussian 92*; Gaussian Inc.: Pittsburgh, PA, 1992. (b) Frisch, A. M. J.; Trucks, G. W.; Schlegel, H. B.; Gill, P. M. W.; Johnson, B. G.; Robb, M. A.; Cheeseman, J. R.; Keith, T. A.; Petersson, G. A.; Montgomery, J. A.; Raghavachari, K.; Al-Laham, M. A.; Zakrzewski, V. G.; Ortiz, J. V.; Foresman, J. B.; Cioslowski, J.; Stefanov, B. B.; Nanayakkara, A.; Challacombe, M.; Peng, C. Y.; Ayala, P. Y.; Chen, W.; Wong, M. W.; Andres, J. L.; Replogle, E. S.; Gomperts, R.; Martin, R. L.; Fox, D. J.; Binkley, J. S.; DeFrees, D. J.; Baker, J.; Stewart, J. J. P.; Head-Gordon, M.; Gonzalez, C.; Pople, J. A. *Gaussian 94*; Gaussian Inc.: Pittsburgh, PA, 1995.

(34) Sakaki, S.; Ieki, M. *J. Am. Chem. Soc.* **1993**, *115*, 2373.

(35) (a) Levy, C. J.; Puddephatt, R. J. *Organometallics* **1995**, *14*, 5019. (b) Levy, C. J.; Puddephatt, R. J. *Organometallics* **1997**, *16*, 4115.

(36) We evaluated the Pt(IV)−SiH_3 bond energy in $Pt(H)(SiH_3)_3(PH_3)_2$, recently. The Pt(IV)−SiH_3 bond energy is similar to the Pt(IV)−SiH_3 bond energy. Sakaki, S.; Kawaguchi, H.; Sugimoto, M. To be published.

Table 2. Pt-H and Pt−SiR_3 (R = H, Cl, or Me) Bond Energies (kcal/mol)

	Pt−H	Pt−SiH_3	Pt−$SiMe_3$	Pt−$SiCl_3$	H−SiH_3	H−$SiMe_3$	H−$SiCl_3$
MP2	56.9	55.6	56.6	70.3	91.0	93.5	92.8
MP3	59.4	53.2	52.8	68.9	93.1	95.7	95.0
MP4DQ	59.2	53.6	53.2	68.8	93.4	95.9	95.3
MP4SDQ	58.8	53.9	53.9	68.5	93.4	95.8	94.9

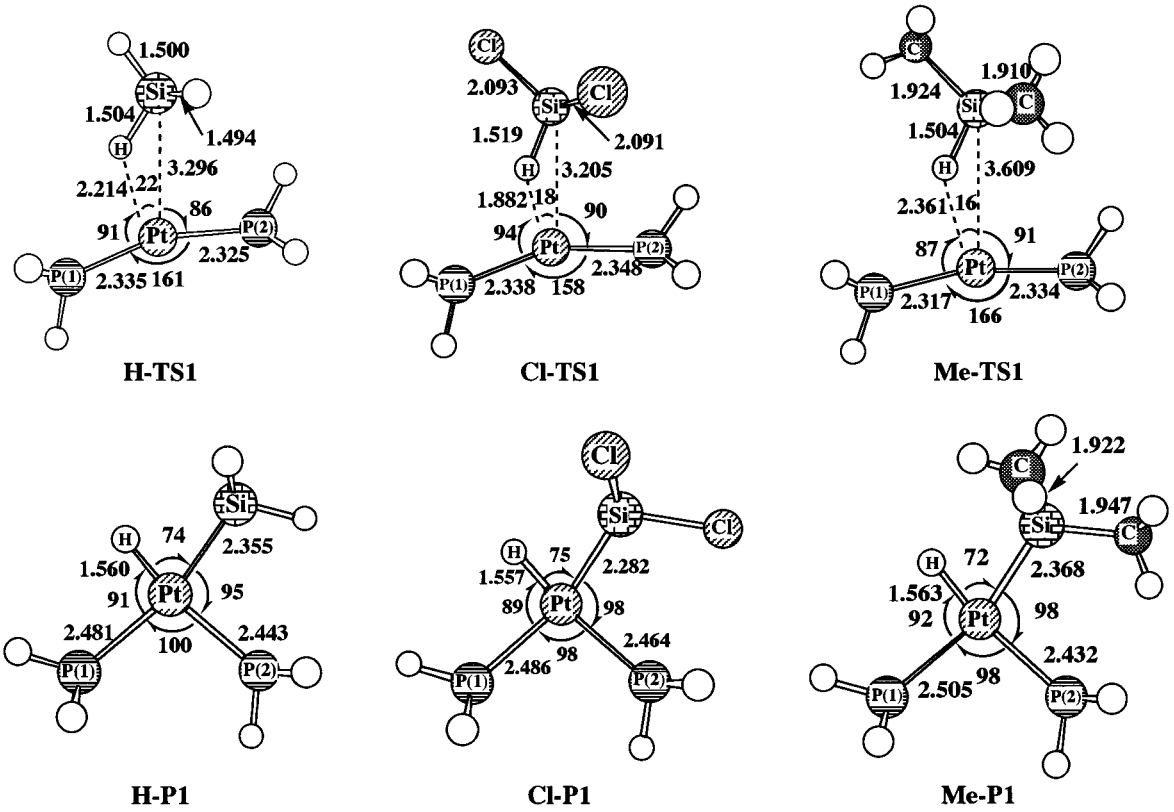

Figure 1. Optimized geometries of the transition state and product in the Si−H oxidative addition of H−SiR_3 (R = H, Cl, or Me) to $Pt(PH_3)_2$. Bond lengths are given in angstroms and bond angles in degrees.

withdrawing substituent strengthens the Pt−silyl bond. As a result, the H−$SiCl_3$ oxidative addition is the most exothermic. On the other hand, the Pt−$SiMe_3$ bond is as strong as the Pt−SiH_3 bond while the oxidative addition of H−$SiMe_3$ is less exothermic than the H−SiH_3 oxidative addition. This is because the Si−H bond of $SiHMe_3$ is slightly stronger than that of SiH_4 (Table 2). Although the reaction energy significantly depends on the substituent on Si, the activation energy is almost the same in the three reaction systems. The reason will be discussed below.

Several interesting differences in the transition-state (TS) structure are found among R = H, Cl, and Me, as shown in Figure 1; for instance, the Pt−H and Pt−Si distances become shorter in the order R = Me > H > Cl. However, the silane moiety distorts little and the Si−H bond that is to be broken in the reaction lengthens little at the TS in all three reaction systems. These features indicate that the transition state seems to be reactant-like, independent upon the substituent introduced on Si. This is the main reason that the activation energy is almost the same in all three reaction systems.

The geometries of the products also exhibit interesting features (Figure 1). The Pt−Si distance becomes longer in the order R = Cl < H < Me. This is consistent with the decreasing order of the Pt−SiR_3 bond energy, R = Cl > H ≈ Me. The Pt−$P^{(1)}$ bond trans to SiR_3 is longer than the Pt−$P^{(2)}$ bond trans to the hydride, which indicates that the trans influence of SiR_3 is stronger than that of the hydride.[34,37] The difference between two Pt−P bond distances is considered a measure of the trans influence difference between hydride and SiR_3. When R = Me, the Pt−$P^{(1)}$ distance is the longest in all of the complexes and, moreover, the difference between the two Pt−P bond distances is the greatest. When R = Cl, the Pt−$P^{(1)}$ bond is ca. 0.02 Å longer than the Pt−$P^{(2)}$ bond. When R = H, the Pt−$P^{(1)}$ bond is 0.07 Å longer than the Pt−$P^{(2)}$ bond. From these results, it is concluded that the trans influence of $SiMe_3$ is the strongest and that of $SiCl_3$ is the weakest. It seems to be inconsistent that the Pt−$SiMe_3$ bond is the weakest but its trans influence is the strongest. However, this seeming inconsistency is not unreasonable if we consider that the trans influence arises from the strong dative interaction of $SiMe_3$ but the Pt−SiR_3 bond energy is determined by a different factor.[38]

Ethylene Insertion into the Pt−H Bond of *cis*-$PtH(SiR_3)(PH_3)(C_2H_4)$. Ethylene insertion was investigated here in a four-coordinate complex, $PtH(SiR_3)(PH_3)(C_2H_4)$, since it is theoretically[39] and experiment-

(37) (a) The strong trans influence of the silyl ligand is reported theoretically[23] and experimentally.[37b] (b) Chatt, J.; Eaborn, C.; Ibekwe, S. D.; Kapoor, P. N. *J. Chem. Soc.* **1970**, 1343.
(38) Sakaki, S.; Mizoe, N.; Sugimoto, M. To be published.
(39) Thorn, D. L.; Hoffmann, R. *J. Am. Chem. Soc.* **1978**, *100*, 2079.

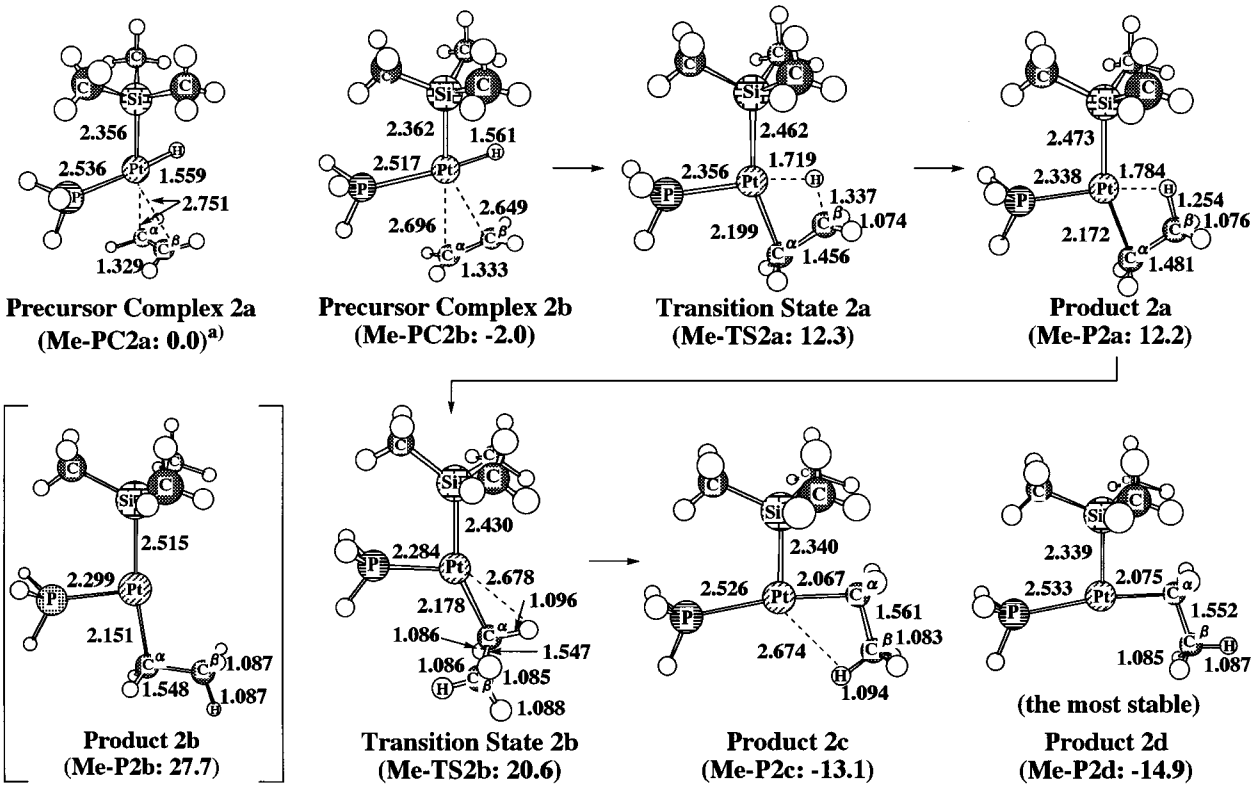

Figure 2. Geometry changes in ethylene insertion into the Pt−H bond of *cis*-PtH($SiMe_3$)(PH_3)(C_2H_4). Bond lengths are given in angstroms and bond angles in degrees.

ally[40−42] believed that ethylene is easily inserted into a metal-hydride bond in a four-coordinate complex but with difficulty in a five-coordinate complex when the central metal takes a d^8 electron configuration. Displacement of phosphine by alkene is not surprising, even in platinum complexes, since Ozawa et al.[19] reported that one phosphine is substituted by alkyne in *cis*-Pt(CH_3)($SiPh_3$)($PMePh_2$)$_2$. The geometry changes of the insertion into the Pt−H bond of PtH($SiMe_3$)(PH_3)(C_2H_4) are shown in Figure 2. Similar geometry changes are observed for R = H and R = Cl, which are given in the Supporting Information. Two structures of the precursor complex were examined; in one (**Me-PC2a**), ethylene is perpendicular to the molecular plane, and in the other (**Me-PC2b**), ethylene is on the molecular plane. **Me-PC2b** is slightly more stable than **Me-PC2a**, while the energy difference is very small (about 2 kcal/mol), as shown in Figure 3.

The transition-state structure **Me-TS2** exhibits various interesting features (Figure 2): (1) the Pt−C^α distance is almost the same as that in the product, (2) the Pt−H^γ distance lengthens slightly to 1.7 Å, (3) the C^β−H^γ distance is still long (1.337 Å), and (4) the C^α−C^β distance is almost intermediate between the reactant and the product. These results clearly demonstrate that the Pt−alkyl bond is almost formed at the TS, preceding

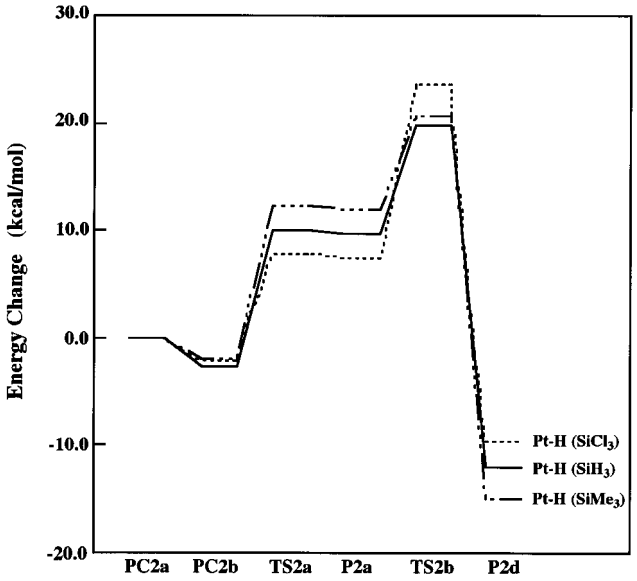

Figure 3. Energy changes upon ethylene insertion into the Pt−H bond of *cis*-PtH($SiMe_3$)(PH_3)(C_2H_4) (kcal/mol at the MP4SDQ level).

Pt−H^γ bond breaking and C^β−H^γ bond formation. This is a characteristic feature generally observed in many insertion reactions of ethylene.[7,43,44] In the product **Me-P2a** just after the insertion, the Pt−H^γ distance is only 1.78 Å, which strongly suggests that the bonding interaction still remains between Pt and H^γ. At the same time, we notice that the C^β−H^γ distance is much

(40) (a) Clark, H. C.; Kurosawa, H. *Inorg. Chem.* **1972**, *11*, 1275. (b) Clark, H. C.; Jablonski, C.; Halpern, J.; Mantovani, A.; Well, T. A. *Inorg. Chem.* **1974**, *13*, 1541. (c) Clark, H. C.; Jablonski, C. R. *Inorg. Chem.* **1974**, *13*, 2213. (d) Clark, H. C.; Wong, C. S. *J. Am. Chem. Soc.* **1974**, *96*, 7213. (e) Clark, H. C.; Jablonski, C. R.; Wong, C. S. *Inorg. Chem.* **1975**, *14*, 1332.

(41) Ben-David, Y.; Portnoy, M.; Gozin, M.; Milstein, D. *Organometallics* **1992**, *11*, 1995.

(42) Ermer, S. P.; Struck, G. E.; Bitler, S. P.; Richards, R.; Bau, R. R.; Flood, T. C. *Organometallics* **1993**, *12*, 2634.

(43) Koga, N.; Obara, S.; Kitaura, K.; Morokuma, K. *J. Am. Chem. Soc.* **1985**, *107*, 7109.

(44) Sakaki, S.; Ohkubo, K. *Organometallics* **1989**, *8*, 2970. Sakaki, S.; Musashi, Y. *Inorg. Chem.* **1995**, *34*, 1914.

Table 3. Activation Energy (E_a)[a] and Reaction Energy (ΔE)[b] of the Ethylene Insertion Into Pt−H and Pt−SiR_3 Bonds (kcal/mol)

	insertion into Pt−H			insertion into Pt−SiR_3		
	E_a(**TS2a**)[a]	E_a(**TS2b**)[b]	ΔE[c]	E_a(**TS3a**)[a]	E_a(**TS3b**)[d]	ΔE[c]
			R = H			
HF	15.6	26.2	−6.7	44.1	15.4	8.6
MP2	9.9	22.7	−5.7	42.8	18.9	10.3
MP3	11.9	22.9	−8.3	41.3	17.0	5.5
MP4DQ	12.6	22.6	−7.2	43.7	20.0	8.0
MP4SDQ	12.7	22.4	−6.7	44.1	20.5	9.0
SD-CI(DS)	12.0	22.4	−7.4			
SD-CI(P)	12.0	22.5	−7.4			
CCD	12.6	22.4	−7.8			
CCD(ST4)	12.2	22.5	−6.7			
			R = Cl			
MP4SDQ	9.8	25.7	−5.4	59.8	9.2	7.0
			R = Me			
MP4SDQ	14.3	22.6	−10.8	44.1	6.7	2.8

[a] E_a = energy difference between the more stable precursor complex (**PC2b** and **PC3b**) and the transition state. [b] E_a(**TS2b**) = energy difference between the precursor complex and **TS2b**. [c] ΔE = energy difference between the product and the precursor complex (a negative value represents the exothermicity). [d] E_a(**TS3b**) = energy difference between **P3a** and **TS2b**.

longer than the usual C−H bond. These features indicate that **Me-P2a** involves a strong agostic interaction between the Pt and H^{γ} atoms. Despite the strong agostic interaction, **Me-P2a** is not the most stable, since two strong silyl and alkyl ligands[37] take positions trans to each other. In **Me-P2b**, the agostic interaction is broken, and therefore, **Me-P2b** is much less stable than **Me-P2a** by 15.5 kcal/mol (MP4SDQ). **Me-P2d** is the most stable, because the coordinating site trans to the silyl ligand is empty. The agostic interaction is not formed in **Me-P2d**, probably because of the strong trans influence of the silyl ligand.

The activation barrier (E_a) and the reaction energy (ΔE) were calculated with various computational methods to examine correlation effects on the insertion reaction. As shown in Table 3, E_a and ΔE fluctuate at the Hartree−Fock (HF), MP2, and MP3 levels to a much lesser extent than those in the oxidative addition (Table 1). Moreover, they change little upon going to CCD-(ST4) from MP4DQ. It should be concluded that electron correlation effects on energy change are not very significant in the insertion reaction unlike those in the oxidative addition.

In the isomerization reaching the most stable product **P2d** from **P2a**, the transition state (**TS2b**) was optimized, as shown in Figure 2. A similar TS was also optimized for R = H and Cl. Since **P2a** is only slightly more stable than **TS2a**, as shown in Figure 3, the activation barrier of the isomerization is defined here as an energy difference between **TS2b** and **PC2b**. Apparently, **TS2b** lies at a much higher energy than **TS2a**. This means that **TS2b** is a real transition state to reach the most stable product **P2d** (see Figure 3). In **TS2b**, the agostic interaction is almost broken and the moving alkyl group overlaps well with the doubly occupied d_{xz} orbital of Pt. The origin of the activation barrier would be attributed to the four-electron repulsion between alkyl sp^3 and Pt d_{xz} orbitals (see Scheme 2);[45] actually, the alkyl sp^3 orbital rises in energy by 3.3 eV for R = H, 3.7 eV for R = Cl, and 3.0 eV for R = Me upon going to **TS2b** from **P2a**.

The relative stabilities of **TS2a**, **P2a**, and **TS2b** are significantly influenced by the substituents on Si (Figure 3). **TS2a** and **P2a** are the least stable for R = Me and the most stable for R = Cl. These substituent effects are interpreted in terms of the trans influence of the silyl ligand. Because the trans influence of SiR_3 becomes stronger in the order R = Cl < H < Me (see above), the Pt−C^{α} distance of **P2a** becomes longer in the order R = Cl (2.126 Å) < H (2.152 Å) < Me (2.172 Å), where the Pt−C^{α} distance is given in parentheses, and **TS2a** and **P2a** become less stable in the order R = Cl < H < Me. The relative stability of **TS2b** is more or less different from that of **TS2a** and **P2a**, as follows; **TS2b** becomes less stable in the order **H-TS2b** ≈**Me-TS2b** < **Cl-TS2b**. This order is interpreted in terms of the four-electron repulsion between the SiR_3 sp^3 and Pt d_{xz} orbitals. The Pt−C^{α} distance of **TS2b** decreases in the order **Me-P2a** (2.178 Å) > **H−P2a** (2.168 Å) > **Cl−P2a** (2.154 Å), reflecting the decreasing order of the Pt−C^{α} distance in **P2a**, where the Pt−C^{α} distance at **TS2b** is given in parentheses. As a result, the four-electron repulsion is the greatest in R = Cl and the weakest in R = Me, because the shorter Pt−C^{α} distance gives rise to the greater four-electron repulsion; in fact, the sp^3 orbital of the alkyl group increases in energy the most in **Cl-TS2b** and the least in **Me-TS2b** (vide supra). Nevertheless, **Me-TS2b** is slightly less stable than **H-TS2b**. This is probably because of the large steric repulsion from $SiMe_3$. Thus, the isomerization easily occurs when SiR_3 exhibits strong trans influence.

The reaction energy, which is defined as the energy difference between **PC2b** and **P2d**, becomes more exothermic in the order R = Cl < H < Me (Table 3). The difference in the reaction energy might be interpreted in terms of the trans influence of SiR_3. The ethylene coordination in **PC2b** is the weakest for R =

Scheme 2

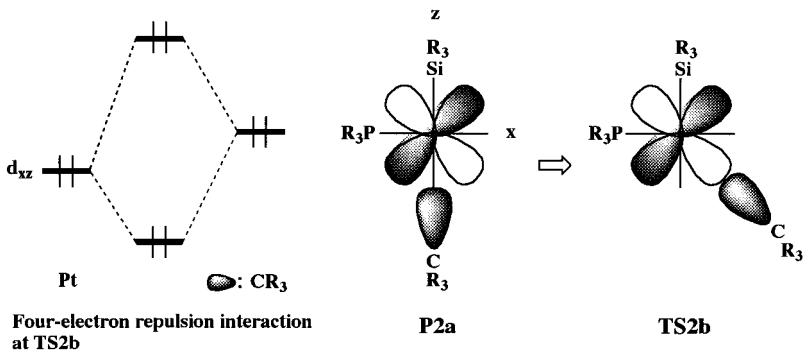

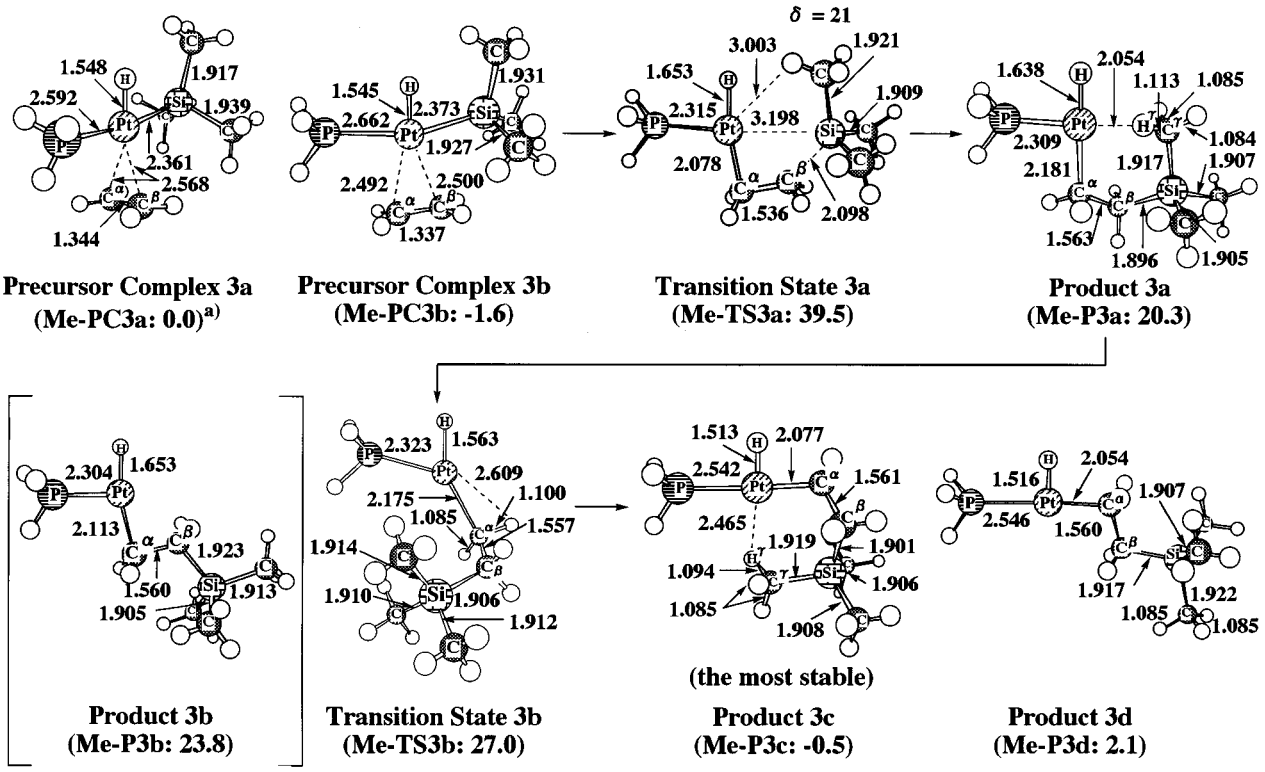

Figure 4. Geometry changes of ethylene insertion into the Pt−$SiMe_3$ bond of *cis*-$PtH(SiMe_3)(PH_3)(C_2H_4)$. Bond lengths are given in angstroms and bond angles in degrees.

Me and the strongest for R = Cl, since the trans influence becomes weaker in the order $SiMe_3$ > SiH_3 > $SiCl_3$. On the other hand, SiR_3 influences the relative stability of **P2d** little, because there is no ligand at a position trans to SiR_3 in **P2d**. Thus, the exothermicity increases in the order R = Cl < H < Me.

Ethylene Insertion into the Pt−SiR_3 Bond of *cis*-$PtH(SiR_3)(PH_3)(C_2H_4)$. The geometry changes of ethylene insertion into the Pt−$SiMe_3$ bond are shown in Figure 4. Similar geometry changes occur in the other two reaction systems. In the precursor complexes, **Me-PC3b** is slightly more stable than **Me-PC3a** (see Figure 5). In the transition state **TS3a**, the Pt−C^{α} distance is almost the same as that in the product, the Pt−Si distance considerably lengthens to 3 Å, and the Si−C^{β} distance is about 2.1 Å, being only 0.2 Å longer than that in the product. These features indicate that the Pt−alkyl and Si−C bonds are almost formed and the Pt−silyl bond is almost broken at the TS. Thus, **TS3a** should be characterized to be product-like.

In the product **Me-P3a** just after the insertion, the Pt−H^{γ} distance is rather short (2.05 Å), the Si−C^{γ} bond is 0.1 Å longer than the usual Si−C bond, and the C^{γ}−H^{γ} bond is 0.03 Å longer than the usual C−H bond. These features suggest that an agostic interaction is formed between Pt and the Me group. Actually, **Me-P3a** is slightly more stable than **Me-P3b**, which does not involve the agostic interaction (see relative energies given in Figure 4). The small stabilization of **Me-P3a** is not surprising because **Me-P3a** is stabilized by the agostic interaction but at the same time destabilized by the steric repulsion arising from three Me groups on Si. The most stable product is **Me-P3c** (see Figure 4), since the coordinating site trans to the strong hydride ligand is empty.

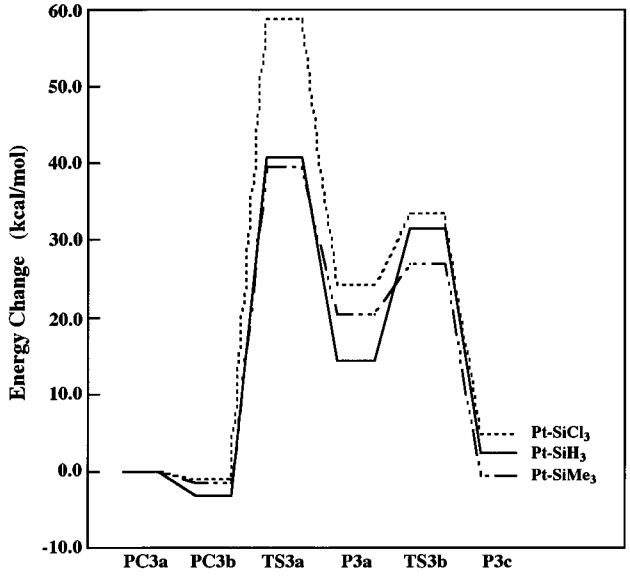

Figure 5. Energy changes upon ethylene insertion into the Pt−SiR_3 bond of *cis*-$PtH(SiMe_3)(PH_3)(C_2H_4)$ (kcal/mol at the MP4SDQ level).

H-P3a and **Cl-P3a** also exhibit similar geometrical features, as shown in Figure 6 (geometries of the other intermediates and TS are given in the Supporting Information). In both, the Pt−H^{γ} and Pt−Cl^{γ} distances are only 1.754 and 2.640 Å, respectively. Consistent with these short distances, the Si−H^{γ} and Si−Cl^{γ} distances are longer than their usual bond distances. These features clearly indicate that **H-P3a** and **Cl-P3a**

(45) (a) If we discuss the energy difference between **P2a** and **TS2b**, we must take into consideration the loss of an agostic interaction. However, the energy difference between **PC2b** and **TS2b** is discussed here. Thus, we do not need to discuss the loss of an agostic interaction.

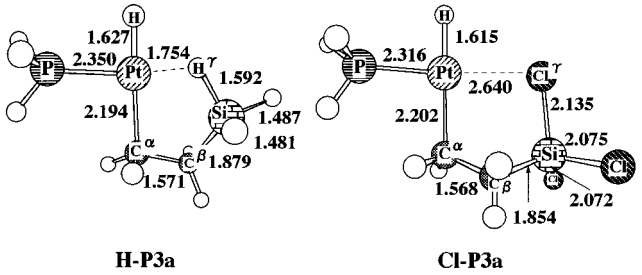

Figure 6. Geometries of the product just after the ethylene insertion into the $Pt-SiR_3$ bond (R = H or Cl). Bond lengths are given in angstroms and bond angles in degrees.

involve the agostic interaction. The agostic interaction in **H−P3a** and **Cl−P3a** is much stronger than that in **Me-P3a**, as clearly shown by the large energy difference between **P3a** and **P3b**: 18.4 kcal/mol for R = H and 14.3 kcal/mol for R = Cl. Previous theoretical studies of $Ti(C_2H_5)(PH_3)(X)_2H$ (X = halogen) and $M(CH_2CH_3)H(PH_3)$ (M = Pd or Pt) clearly demonstrated that the agostic interaction is formed through the charge-transfer interaction between the empty d orbital of the metal and the C−H occupied orbital.[43,46] The H atom of the Me group is less negatively charged than the Cl and H of the silyl group because of the large electronegativity of C. Thus, **H−P3a** and **Cl−P3a** have a stronger agostic interaction than **Me-P3a**. Despite the agostic interaction, **H−P3a** and **Cl−P3a** are not the most stable. The most stable products are **H−P3c** and **Cl−P3c** in which the coordinating site trans to the hydride is empty, like in **Me-P3d**.

The isomerization from **P3a** to **P3c** occurs through **TS3b**, as shown in Figure 4. In **TS3b**, the agostic interaction is almost broken and the $CH_2CH_2SiR_3$ group overlaps well with the doubly occupied d_{xz} orbital of Pt, like that in **TS2b**. Since **P3a** is much more stable in energy than **TS3a**, **P3a** is considered to be an intermediate, and therefore, the activation barrier for the isomerization **P3a** → **P3c** is evaluated as an energy difference between **P3a** and **TS3b**. In this case, the origin of the barrier would be attributed to the breaking of the agostic interaction and the four-electron repulsion between alkyl sp^3 and Pt d_{xz} orbitals; actually, the alkyl sp^3 orbital increases in energy by ca. 3 eV upon going to **TS3b** from **P3a**, independent of the substituent on Si. The difference in the barrier among R = H, Cl, and Me arises from the agostic interaction in **P3a**; since the agostic interaction was calculated to decrease in the order R = H > Cl > Me (see above), the barrier of the isomerization becomes higher in the order Me < Cl < H, as shown in Table 3. Though the barrier depends on the substituent on Si, all of these barriers are much lower in energy than the barrier of the ethylene insertion into $Pt-SiR_3$, as shown in Table 3 and Figure 5. This means that the real barrier exists at **TS3a** of the ethylene insertion.

Why does the ethylene insertion into the Pt−H bond occur more easily than the insertion into the $Pt-SiR_3$ bond? As noted above, the ethylene insertion into the Pt−silyl bond requires a significantly higher activation barrier (see Figure 5). It is worthwhile to investigate the reason that the insertion into the Pt−H bond occurs more easily than the insertion into the $Pt-SiH_3$ bond. Here, we examined two factors to clarify the reason for this difference. The first is the bond energy. In the ethylene insertion into the Pt−H bond, the Pt−H bond is lost while Pt−alkyl and C−H bonds are formed, as shown in Scheme 3. In the insertion into the $Pt-SiR_3$ bond, the $Pt-SiR_3$ bond is lost while Pt−alkyl and Si−C bonds are formed. Although the Pt−H bond is as strong as the $Pt-SiH_3$ bond, the C−H bond is much stronger than the Si−C bond. Thus, it should be reasonably concluded that insertion into the Pt−H bond more favorably occurs than that into the $Pt-SiH_3$ bond from thermodynamic point of view. In particular, insertion into the $Pt-SiCl_3$ bond needs a much higher activation barrier than the others. This would arise from the fact that the $Pt-SiCl_3$ bond is the strongest in $Pt-SiR_3$ (R = H, Cl, or Me), as shown in Table 2. However, insertion into the $Pt-SiMe_3$ bond requires a higher activation barrier than insertion into the $Pt-SiH_3$ bond, whereas the $Pt-SiMe_3$ bond is as strong as the $Pt-SiH_3$ bond. This would arise from the steric effects of three methyl groups of $SiMe_3$.

The next factor to be investigated is the bonding nature at the TS. As discussed previously,[7,44] the hydride can form a new bonding interaction with ethylene, keeping the Pt−H bond, because of its spherical 1s valence orbital. On the other hand, SiR_3 can start to form a new bonding interaction with ethylene only when SiR_3 changes its direction toward ethylene, because of its directional sp^3 valence orbital. Such a direction change weakens the $Pt-SiR_3$ bond and destabilizes the TS. As a result, ethylene insertion into the $Pt-SiR_3$ bond requires a much higher activation barrier. This is a plausible reason, and in fact, a similar discussion based on the directional sp^3 valence orbital

Scheme 3. Bond Energies of Ethylene Insertion (kcal/mol MP4SDQ Level)

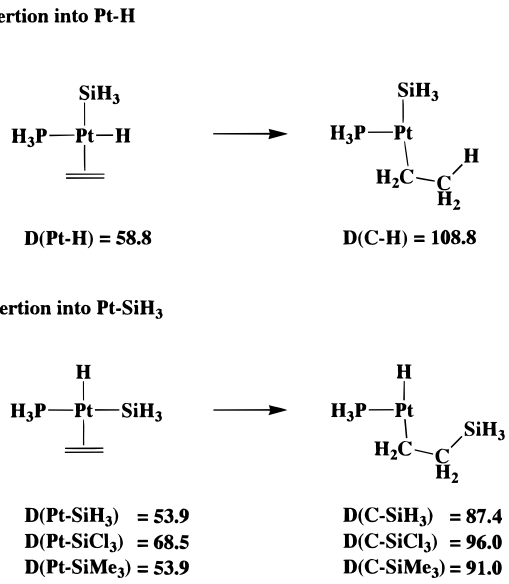

(46) (a) Koga, N.; Obara, S.; Morokuma, K. *J. Am. Chem. Soc.* **1984**, *106*, 4625. (b) Obara, S.; Koga, N.; Morokuma, K. *J. Organomet. Chem.* **1984**, *270*, C33. (c) Koga, N.; Morokuma, K. *J. Am. Chem. Soc.* **1988**, *110*, 108.

(47) Blomberg, M. R. A.; Brandemark, U.; Siegbahn, P. E. M. *J. Am. Chem. Soc.* **1983**, *105*, 5557.

(48) Saillard, J. Y.; Hoffmann, R. *J. Am. Chem. Soc.* **1984**, *106*, 2006.

Scheme 4. Distortion Energies in Ethylene Insertion (MP4SDQ level; kcal/mol)

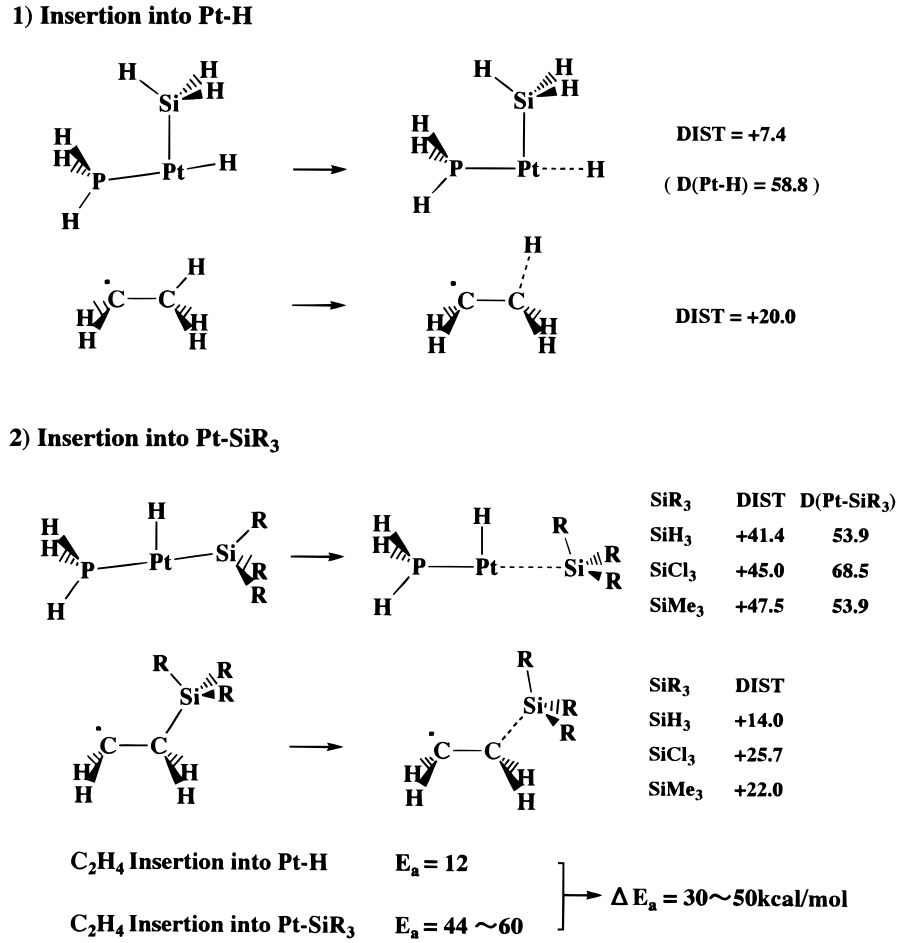

of CH_3 was previously presented to explain why the H−CH_3 and CH_3−CH_3 oxidative additions require a higher activation energy than the H−H oxidative addition.[34,47−49] However, no clear evidence has been presented to our knowledge. We examined the distortion energy (DIST) that is necessary to deform Pt(H)(SiH_3)(PH_3), •CH_2CH_2H, and •$CH_2CH_2SiH_3$ from their equilibrium geometries to the distorted geometries taken in the TS. As shown in Scheme 4, DIST of •CH_2-CH_2H is 20 kcal/mol in the insertion into the Pt−H bond and that of •$CH_2CH_2SiR_3$ is 14−26 kcal/mol in the insertion into the Pt−SiR_3 bond. These two DISTs are similar to each other. However, DIST of Pt(H)(SiR_3)-(PH_3) is significantly different between the two insertion reactions. It is evaluated to be 7.4 kcal/mol for the insertion into the Pt−H bond and over 40 kcal/mol for the insertion into the Pt−SiR_3 bond. Moreover, the difference in DIST of PtH(SiR_3)(PH_3) between these two insertion reactions roughly corresponds to the E_a difference between the two insertions (see Table 3). As shown in Scheme 4, DIST of PtH(SiR_3)(PH_3) corresponds to about 80% of the Pt−SiR_3 bond energy. This means that the Pt−SiR_3 bond is about 80% broken at the TS. These results provide us a clear conclusion: in the ethylene insertion into the Pt−SiR_3 bond, the SiR_3 group should change its direction toward ethylene because of the directional sp^3 valence orbital of SiR_3, which causes the much larger distortion of PtH(SiR_3)(PH_3) and leads to the considerably higher activation barrier than that of the insertion into the Pt−H bond (remember that DIST of PtH(SiR_3)(PH_3) is small in the insertion into Pt−H).

Electronic Process of Ethylene Insertion. Here, we also mention the characteristic feature of the ethylene insertion into the Pt−SiR_3 bond. At the TS of the insertion into the Pt−H bond, the C^α atom interacting with Pt becomes more negatively charged but the C^β atom interacting with H (hydride) becomes less negatively charged, as shown by NBO charges[50] at the transition state (see Scheme 5). This electron distribution is easily interpreted in terms of orbital mixing in the HOMO: the hydride 1s orbital interacts with the ethylene π^* orbital in a bonding way into which the ethylene π orbital mixes in an antibonding way with the hydride 1s orbital (Scheme 5C), since the ethylene π orbital lies at a lower energy than the hydride 1s orbital. As a result, the C^α p_π contribution is enhanced but the C^β p_π contribution is reduced in the HOMO to yield the greater negative charge on C^α than that on C^β. A similar orbital mixing was reported in the ethylene insertion into Cu(I)−H and Cu(I)−CH_3 bonds.[44] At the TS of the insertion into the Pt−SiR_3 bond, on the other hand, the C^β atom is more negatively charged than the C^α atom, as shown in Scheme 5B. The nature of the HOMO is similar to that of the insertion into the Pt−H bond; for instance, the C^β p_π coefficient is smaller

(49) (a) Low, J. J.; Goddard, W. A. *Organometallics* **1986**, *5*, 609. (b) Low, J. J.; Goddard, W. A. *J. Am. Chem. Soc.* **1986**, *108*, 6115.

(50) Reed, A. E.; Curtis, L. A.; Weinhold, F. *Chem. Rev.* **1988**, *88*, 849 and references therein.

Scheme 5

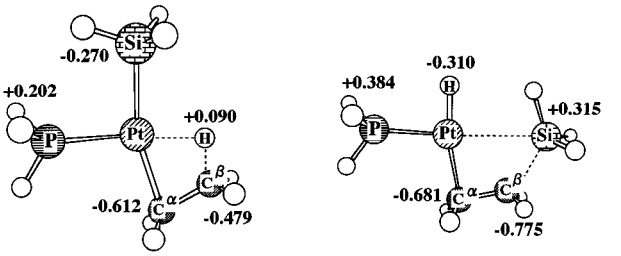

(A) NBO charges[a] at transition state of ethylene insertion into Pt–H bond

(B) NBO charges[a] at transition state of ethylene insertion into Pt–SiH_3 bond

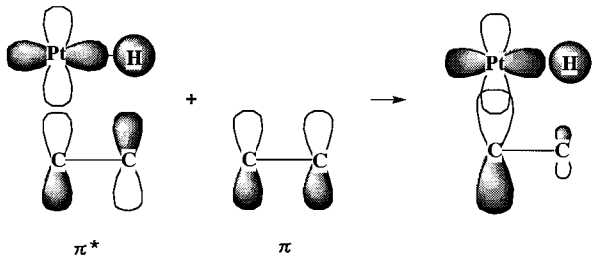

π^* π

(C) Orbital mixing at HOMO

than the C^α p_π coefficient in the HOMO. Thus, the electron distribution does not arise from the feature of the HOMO. An important difference between these two insertion reactions is attributed to the electron populations of the SiR_3 and H ligands: the SiR_3 ligand is much more positively charged at the transition state than the hydride ligand, probably because of the small electronegativity of Si. The considerably large positive charge on SiR_3 causes σ-polarization of ethylene, making C^β more negatively charged than C^α, and this polarization overcomes the electron distribution of the HOMO. This seems to be a characteristic feature of ethylene insertion into the Pt−SiR_3 bond,[51] and it arises from the smaller electronegativity of SiR_3.

Si−C Reductive Elimination of *cis*-Pt(CH_3)(SiH_3)(PH_3)(L) and C−H Reductive Elimination of *cis*-PtH(CH_3)(PH_3)(L) (L = PH_3 or C_2H_4). Because a d^8 metal tends to have a four-coordinate planar structure, we examined the reductive elimination of four-coordinate complexes Pt(CH_3)(SiR_3)(PH_3)$_2$ and PtH(CH_3)(PH_3)$_2$. As shown in Figure 7, the transition state of Si−C reductive elimination takes a nonplanar structure (geometry changes for R = H and Cl are given in the Supporting Information). A similar nonplanar TS structure was calculated in the oxidative addition of B−B[52] and C−C bonds[38] to Pt(PH_3)$_2$, recently. On the other hand, the TS of the C−H reductive elimination is planar.

The C−H reductive elimination (E_a = 18 kcal/mol) proceeds more easily than the Si−C reductive elimination (E_a = 24 kcal/mol), as shown in Table 4. As discussed previously, the difference is also interpreted in terms of the directional sp^3 valence orbital of SiR_3.[34,47−49] Also, the Si−C reductive elimination is less favorable than the C−H reductive elimination from a thermodynamic point of view. As shown in Scheme 6, the Pt−H and Pt−CH_3 bonds are lost and the C−H bond is formed in the C−H reductive elimination while the Pt−SiR_3 and Pt−CH_3 bonds are lost and the Si−C bond is formed in the SiH_3−CH_3 reductive elimination. Although the Pt−H bond is as strong as the Pt−SiH_3 and Pt−$SiMe_3$ bonds and weaker than the Pt−$SiCl_3$ bond, the C−H bond is stronger than the SiR_3−CH_3 bond by 10−20 kcal/mol and the Pt−CH_3 bond is weaker than the Pt−SiR_3 bond by 13−28 kcal/mol. Thus, the C−H reductive elimination is more favorable than the SiR_3−CH_3 reductive elimination from both the thermodynamic and kinetic points of view.

The activation barrier of the Si−C reductive elimination is not sensitive to the substituent on Si (Table 4). For instance, the $SiCl_3$−CH_3 reductive elimination occurs with a similar activation barrier to that of the SiH_3−CH_3 reductive elimination, whereas the $SiCl_3$−CH_3 bond is 10 kcal/mol stronger than the SiH_3−CH_3 bond (Scheme 6). In this case, the strong $SiCl_3$−CH_3 bond is formed but the strong Pt−$SiCl_3$ bond is broken. The stabilization by the $SiCl_3$−CH_3 bond formation almost compensates for the destabilization by the Pt−$SiCl_3$ bond breaking. Thus, the barrier of $SiCl_3$−CH_3 reductive elimination is similar to that of the SiH_3−CH_3 reductive elimination. The $SiMe_3$−CH_3 reductive elimination occurs with a slightly lower activation barrier than the SiH_3−CH_3 reductive elimination. This is probably because the $SiMe_3$−CH_3 bond is somewhat stronger than the SiH_3−CH_3 bond (see Table 2 and remember that the Pt−$SiMe_3$ bond is as strong as the Pt−SiH_3 bond).

Recently, Ozawa and collaborators experimentally found that the Si−C reductive elimination occurs more easily in *cis*-Pt(CH_3)($SiPh_3$)($PMePh_2$)(alkyne) than in *cis*-Pt(CH_3)($SiPh_3$)($PMePh_2$)$_2$.[19] Since ethylene exists in excess under catalytic reaction conditions, ethylene might coordinate to Pt(H)(R)(PH_3) and Pt(CH_3)(SiR_3)(PH_3). The ethylene coordination yields a stabilization of 15.6 kcal/mol in Pt(CH_3)(SiH_3)(PH_3) and 22.6 kcal/mol in Pt(H)(CH_3)(PH_3), while the stabilization energy by PH_3 coordination is 19.3 kcal/mol for Pt(CH_3)(SiH_3)(PH_3) and 25.3 kcal/mol for Pt(H)(CH_3)(PH_3). These results suggest that ethylene coordination to Pt(CH_3)(SiH_3)(PH_3) and Pt(H)(CH_3)(PH_3) is considered to take place, since the stabilization energy is only slightly different between ethylene and PH_3 coordinations. Thus, we also examined the Si−C reductive elimination in Pt(CH_3)(SiR_3)(PH_3)(C_2H_4) and the C−H reductive elimination in Pt(H)(CH_3)(PH_3)(C_2H_4). The geometry changes are shown in Figure 8. At the transition state (**TS6** and **TS7**), the ethylene C=C bond and the Pt−P bond are almost on the same plane. In the C−H reductive elimination, the C−H bond is also on this plane, like that in **TS5**, while in the Si−C reductive elimination the Si−C bond is almost perpendicular to this plane, like that in **TS4**. The Pt−Si and Pt−C distances of **TS6** are slightly longer than those of **TS4**, and the Si−C distance of **TS6** is slightly shorter than that of **TS4**. Also, the Pt−H and Pt−C distances of **TS7** are slightly longer than those of **TS5**, and the C−H distance of **TS7** is slightly shorter than that of **TS5**. These features indicate that **TS6** and **TS7** are more product-like than **TS4** and **TS5**.

(51) A similar electron distribution was calculated in the ethylene insertion into Pd−$SiCl_3$ of Pd(H)($SiCl_3$)(PH_3)(C_2H_4) and Rh−SiH_3 of Rh(H)(SiH_3)Cl(PH_3)$_2$: Sakaki, S.: Kanechika, T.; Sumimoto, S.; Sugimoto, M. To be published.

(52) Qiang, C.; Musaev, D. G.; Morokuma, K. *Organometallics* **1997**, *16*, 1355.

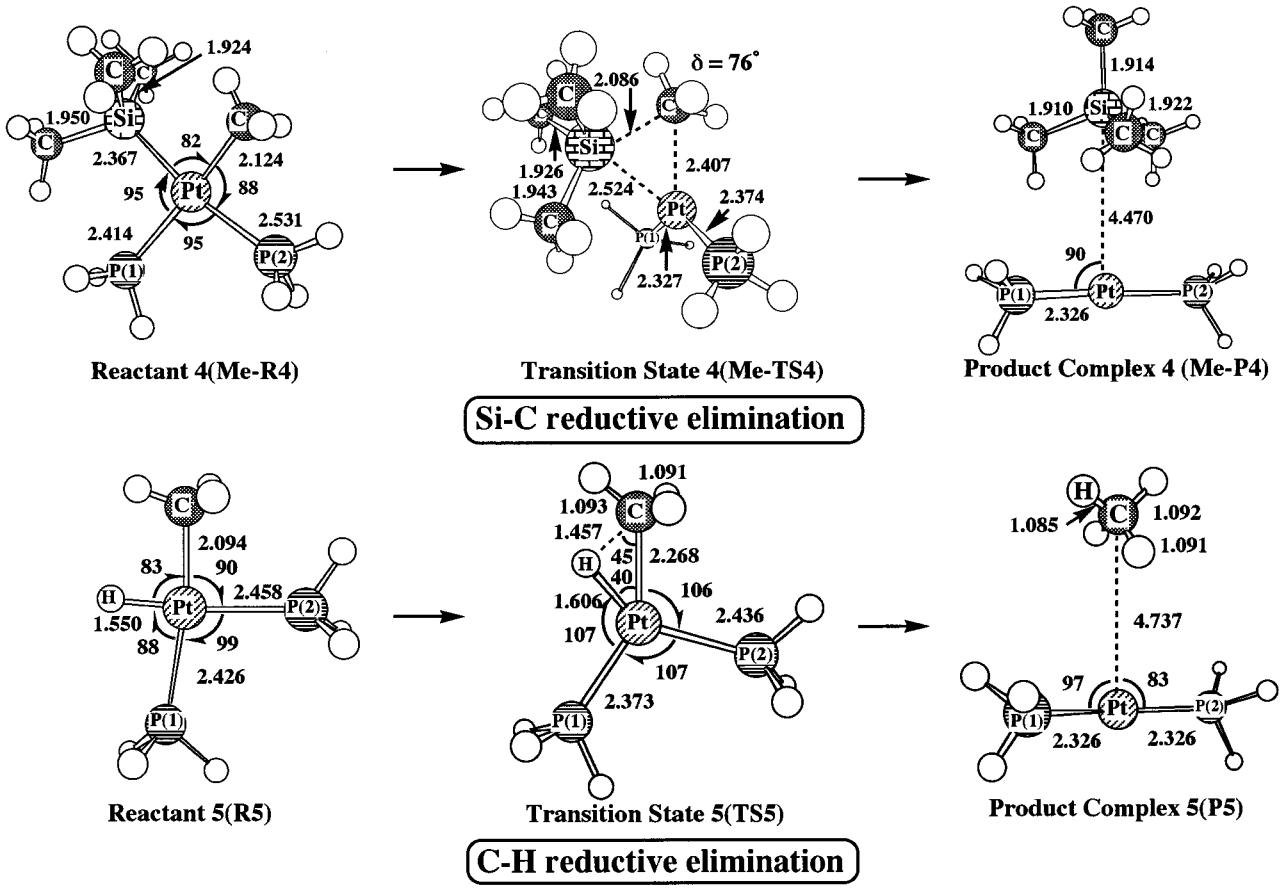

Figure 7. Geometry changes of the Si−C reductive elimination of *cis*-Pt(CH_3)($SiMe_3$)(PH_3)$_2$ (upper) and the C−H reductive elimination of *cis*-PtH(CH_3)(PH_3)$_2$ (lower). Bond lengths are given in angstroms and bond angles in degrees.

Table 4. Activation Energy (E_a)[a] and Reaction Energy (ΔE)[b] of Si−C and C−H Reductive Eliminations (kcal/mol)

	SiH_3-CH_3		$SiCl_3-CH_3$		$SiMe_3-CH_3$		$H-CH_3$	
	E_a[a]	ΔE[b]	E_a[a]	ΔE[b]	E_a[a]	ΔE[b]	E_a[a]	ΔE[b]
(a) Pt(CH_3)(SiR_3)(PH_3)$_2$ or Pt(H)(CH_3)(PH_3)$_2$								
HF	30.4	−11.1	32.8	−4.2	26.8	−19.3	22.5	−24.2
MP2	24.3	8.0	25.2	13.3	21.9	3.2	17.2	−7.3
MP3	28.5	3.7	28.6	9.9	25.6	−1.9	21.7	−9.0
MP4DQ	26.3	4.5	27.4	10.1	24.0	−1.0	19.3	−9.9
MP4SDQ	24.3	4.7	25.8	10.3	22.1	−0.5	17.7	−10.1
(b) Pt(CH_3)(SiR_3)(PH_3)(C_2H_4) or Pt(H)(CH_3)(PH_3)(C_2H_4)								
MP4SDQ	11.1	2.7	11.5	7.6	6.8	−2.4	9.9	−11.0

[a] E^a= energy difference between the reactant and the transition state. [b] ΔE = energy difference between the reactant and the product (a negative value represents the exothermicity).

Scheme 6. Bond Energies (MP4SDQ level, kcal/mol) of Reductive Elimination

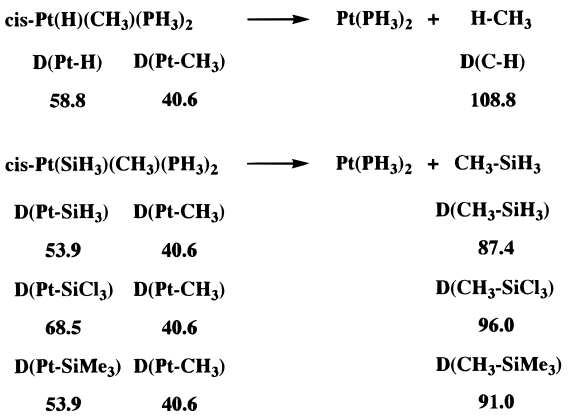

The Si−C reductive elimination of *cis*-Pt(CH_3)(SiR_3)(PH_3)(C_2H_4) and the C−H reductive elimination of *cis*-Pt(H)(CH_3)(PH_3)(C_2H_4), however, occur with a lower activation barrier than the Si−C and C−H reductive eliminations of diphosphine systems Pt(CH_3)(SiR_3)(PH_3)$_2$ and Pt(H)(CH_3)(PH_3)$_2$, respectively, as shown in Table 4. To determine the reason, we investigated the NBO population,[50] as shown in Table 5. Apparently, the NBO population of C_2H_4 increases more at **TS6** and **TS7** than that of PH_3 at **TS4** and **TS5**. This result clearly indicates that C_2H_4 accepts Pt d electrons more easily than PH_3, which would favor the reductive elimination since platinum(II) changes into Pt(0) in the reaction. Actually, the C_2H_4 π^* orbital interacts directly with the Pt d orbital, which is destabilized in energy by the antibonding interaction with the PH_3 lone pair orbital, as shown in Scheme 7. PH_3 cannot form this π-back-bonding interaction because of the lack of a good acceptor orbital. Thus, ethylene stabilizes the transition state of reductive elimination. The above analysis provides a clear explanation for the experimental finding of Ozawa et al. that coordination of an electron-withdrawing alkyne to Pt(II) accelerates the Si−C reductive elimination of Pt(II) complex.[19]

At the end of this section, we will mention whether Pt(CH_3)(SiR_3)(PH_3)L and PtH(CH_3)(PH_3)L are reasonable models for investigation of $SiR_3-CH_2CH_3$ and $H-CH_2CH_2SiR_3$ reductive eliminations, since Pt(C_2H_5)(SiR_3)(PH_3)L and PtH($CH_2CH_2SiR_3$)(PH_3)L undergo

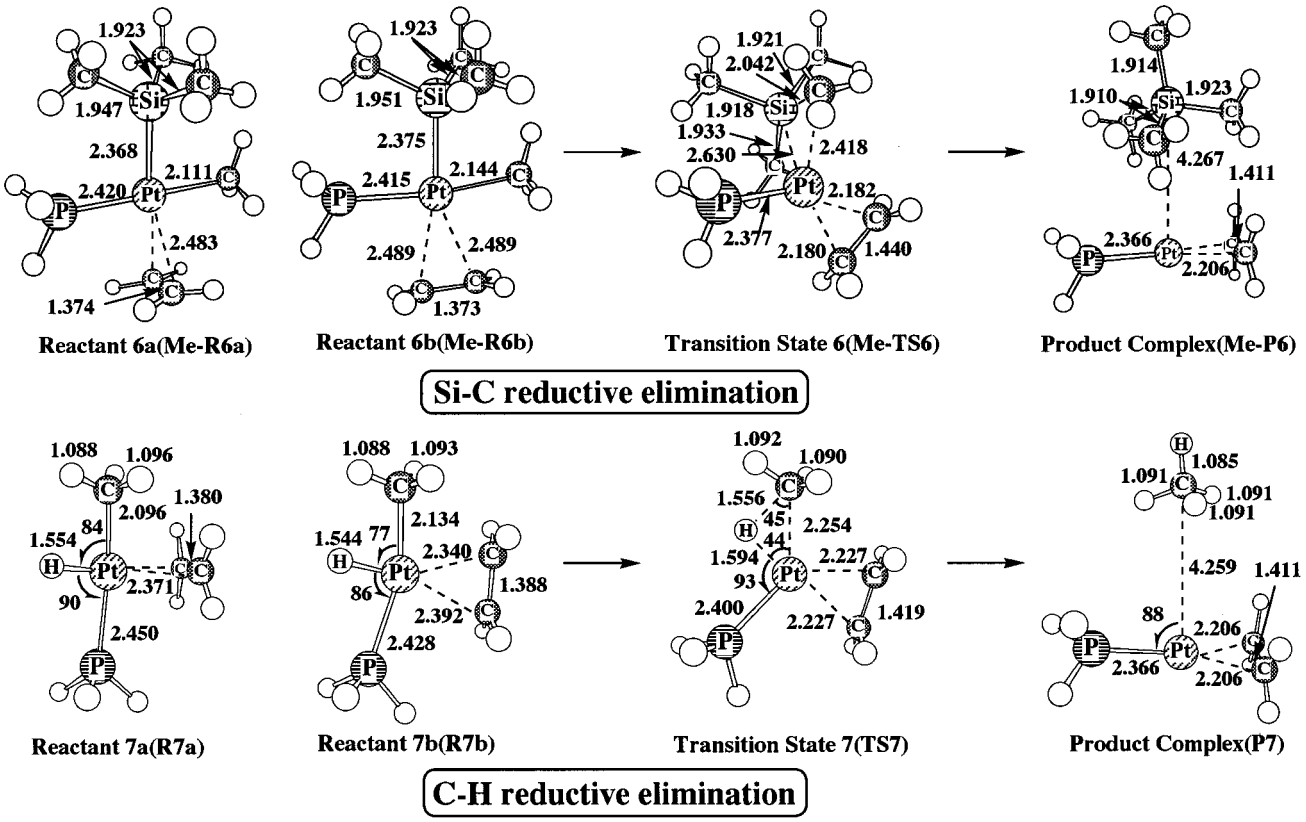

Figure 8. Geometry changes of the Si−C reductive elimination of *cis*-Pt(CH_3)($SiMe_3$)(PH_3)(C_2H_4) (upper) and the C−H reductive elimination of *cis*-PtH(CH_3)(PH_3)(C_2H_4) (lower). Bond lengths are given in angstroms and bond angles in degrees.

Table 5. NBO Population Changes[a] at the Transition State of Si−C and C−H Reductive Elimination

	Pt(CH_3)(SiH_3)(PH_3)$_2$	Pt(CH_3)(SiH_3)(PH_3)(C_2H_4)	Pt(H)(CH_3)(PH_3)$_2$	Pt(H)(CH_3)(PH_3)(C_2H_4)
Pt	0.039	−0.091	0.070	−0.014
SiR_3 or H	−0.188	−0.260	−0.136	−0.133
CH_3	0.013	0.022	−0.085	−0.102
PH_3(1)	0.080	0.040	0.065	0.008
PH_3(2) or C_2H_4	0.057	0.289	0.084	0.239

[a] Reference 50. A positive value means an increase in population and vice versa.

Scheme 7. π-Back-Bonding Interaction between the Pd d and C_2H_4 π^* Orbital

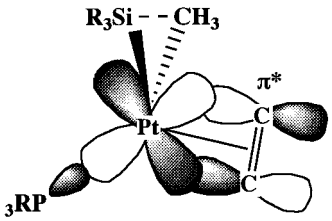

$SiR_3-CH_2CH_3$ and $H-CH_2CH_2SiR_3$ reductive eliminations, respectively, in the real hydrosilylation of ethylene. Their transition states of the Si−C and C−H reductive eliminations were optimized under the constraint that Pt−C−C and Pt−C−C−Si have a staggered structure, where PH_3 was adopted for L to save the CPU time.

This constraint seems reasonable since CH_2CH_3 and $CH_2CH_2SiR_3$ would rotate easily and the assumed geometries suffer the least from the steric repulsion. The transition-state structures and activation barriers for $SiR_3-CH_2CH_3$ and $H-CH_2CH_2SiR_3$ reductive eliminations are similar to those for the SiR_3-CH_3 and $H-CH_3$ reductive eliminations, as shown in Figure 9. Thus, the Si−C and C−H reductive eliminations are considered to be reliably investigated here with Pt(CH_3)(SiH_3)-(PH_3)L and Pt(H)(CH_3)(PH_3)L.

Comparison of Our Results with Experimental Results of Trogler et al. We will mention here a comparison of our results with the experimental results by Prignato and Trogler.[16] In their experiment, the reaction rate is first order in silane concentration but is independent of alkene concentration. Our results indicate that the rate-determining step is the isomerization of the ethylene insertion product. This would suggest that the reaction rate is first order in ethylene, which seemingly disagrees with the experimental results. However, this disagreement would disappear if we consider the hydrosilylation occurs according to eq 9; in eq 9, the equilibrium is reasonably adopted, since

$$\mathrm{Pt(PR_3)_2(alkene)+H-SiR_3} \underset{k_{-1}}{\overset{k_1}{\rightleftharpoons}} \mathrm{Pt(H-SiR_3)(PR_3)_2+alkene} \xrightarrow{k_p} \mathrm{product} \quad (9)$$

alkene more easily interacts with Pt than silane. The reaction rate is represented by eq 10a, as suggested by our results. Equation 10a is changed into eq 10b

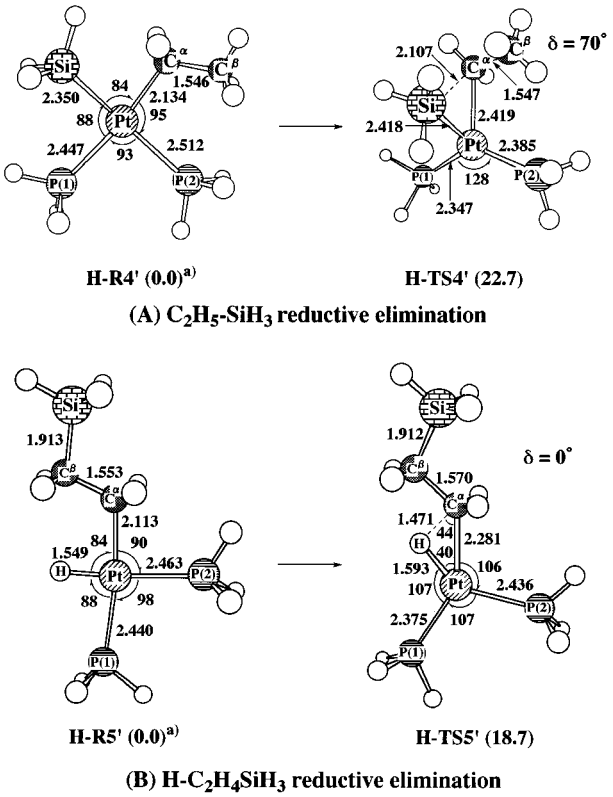

Figure 9. Geometry changes of (A) $SiH_3-C_2H_5$ reductive elimination of *cis*-$Pt(SiH_3)(C_2H_5)(PH_3)_2$ and (B) $H-C_2H_4$-SiH_3 reductive elimination of *cis*-$Pt(H)(C_2H_4SiH_3)(PH_3)$. Bond lengths are given in angstroms and bond angles in degrees. The relative energies are given in parentheses (kcal/mol; MP4SDQ. The staggered structure was assumed in the $Pt-CH_2-CH_3$ and $Pt-CH_2-CH_2-SiH_3$ fragments).

$$\text{rate} = k_p[Pt(H-SiR_3)(PH_3)_2][\text{alkene}] \quad (10a)$$

$$= k_1k_p/\{k_{-1}[\text{alkene}] + k_1\}[Pt(H-SiR_3)(\times \text{alkene})][H-SiR_3][\text{alkene}] \quad (10b)$$

through steady-state approximation of the concentration applied to $[Pt(H-SiR_3)(PR_3)_2]$. Here, we can reasonably assume that k_{-1} is much larger than k_1, since alkene coordinates to Pt much more strongly than silane. As a result, k_1 is neglected in the denominator of eq 10b and eq 11 is obtained. The equation shows that the rate

$$\text{rate} = (k_1k_p/k_{-1}[\text{alkene}])[Pt(H-SiR_3)(\text{alkene})] \times [H-SiR_3][\text{alkene}]$$

$$=(k_1k_p/k_{-1})[Pt(H-SiR_3)(\text{alkene})][H-SiR_3] \quad (11)$$

is first order in silane concentration but independent of alkene concentration, which agrees with the result of Trogler et al. Originally, the alkene concentration was involved in eq 10a, as expected, but this term is finally canceled by the alkene concentration involved in the denominator of eq 11. The next issue is to determine which is the rate-determining step, the alkene dissociation or the isomerization of the insertion product. Our previous calculations indicated that ethylene coordination to $Pt(PH_3)_2$ yields a stabilization

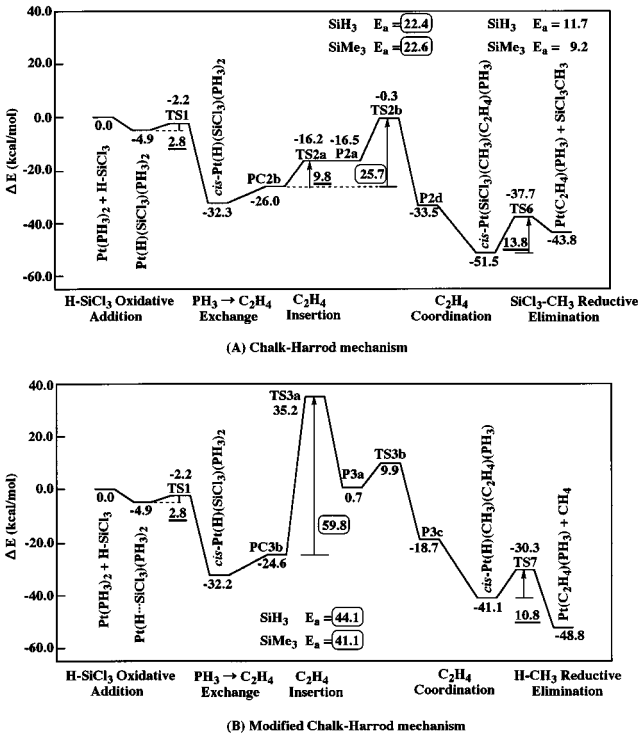

Figure 10. Energy changes along the (A) Chalk−Harrod and (B) modified Chalk−Harrod mechanisms (kcal/mol at the MP4SDQ level).

energy of 20 kcal/mol.[54] This value is slightly smaller than the barrier of the isomerization. Although a more detailed and careful examination would be necessary, the rate-determining step is reasonably concluded to be the isomerization of the ethylene insertion product. More important is that the reaction rate is given by eq 11, independent of whether any rate-determining step is involved in k_p or not. Thus, our conclusion is not inconsistent with the results of Prignato and Trogler. The other important point is that the reaction mechanism is determined by elementary steps involved in the k_p step. This is the reason that our investigation is focused on the k_p step.

Conclusion Concerning the Reaction Mechanism and Prediction for a Good Catalyst. Now, we have completed all of the preparations for making a comparison between Chalk−Harrod and modified Chalk−Harrod mechanisms. In Figure 10A, the energy change along the catalytic reaction is given for R = Cl (energy changes for R = H and Me are given in the Supporting Information).[53] In a Chalk−Harrod mechanism, the rate-determining step is the isomerization of the ethylene insertion product $Pt(SiR_3)(C_2H_5)(PH_3)$ and its barrier is 22 kcal/mol for R = H, 26 kcal/mol for R = Cl, and 23 kcal/mol for R = Me.

In a modified Chalk−Harrod mechanism (Figure 10B), the rate-determining step is the ethylene insertion, independent of the kind of substituent on Si; E_a =

(53) In Figure 10A, the energy change upon going to **PC2b** from **P1** corresponds to the energy change by the following equation: *cis*-$Pt(H)(SiR_3)(PH_3)_2 + C_2H_4 \rightarrow Pt(H)(SiR_3)(PH_3)(C_2H_4) + PH_3$. The energy change upon going to **R5a** from **P2c** corresponds to the energy change by the following equation: $Pt(SiR_3)(CH_3)(PH_3) + C_2H_4 \rightarrow Pt(SiR_3)(CH_3)(PH_3)(C_2H_4)$, since $Pt(SiR_3)(C_2H_5)(PH_3)$ was modeled by $Pt(SiR_3)(CH_3)(PH_3)$ in the Si−C reductive elimination. Figure 10B was drawn in a similar way.

(54) Sakaki, S.; Ieki, M. *Inorg. Chem.* **1991**, *30*, 4218.

44 kcal/mol for R = H and Me and 60 kcal/mol for R = Cl. These activation barriers are much higher than that of the rate-determining step of the Chalk−Harrod mechanism. Thus, it should be clearly concluded that the platinum(0)-catalyzed hydrosilylation of ethylene proceeds through the Chalk−Harrod mechanism.

In platinum−phosphine complexes, the turnover numbers are not high very often.[16] Thus, the calculated activation barrier of 22−26 kcal/mol for the rate-determining step seems consistent with those turnover numbers.

To find a good platinum catalyst, an attempt must be made to lower the activation barrier of the isomerization of the ethylene insertion product since the rate-determining step is the isomerization of the ethylene insertion product. The origin of the activation barrier is the four-electron repulsion between the Pt d_{xz} and alkyl sp^3 orbitals. The four-electron repulsion becomes weak when the Pt d_{xz} orbital is at a low energy. Thus, a π-back-bonding ligand is expected to be favorable for this isomerization, since the π-back-bonding interaction stabilizes the Pt d_{xz} orbital in energy. For instance, phosphite is a reasonable candidate for a good ligand.

Acknowledgment. This work was supported in part by the Ministry of Education, Culture, Sports, and Science through Grants-in Aid for Scientific Research on the Priority Area of Inter-element Chemistry (Grant No. 09239105).

Supporting Information Available: Optimized geometries of ethylene insertion into Pt−H and Pt−SiR_3 of *cis*-PtH(SiR_3)(PH_3)(C_2H_4) (R = H or Cl), the C−H reductive elimination of PtH(CH_3)(PH_3)$_2$, the Si−C reductive elimination of Pt(CH_3)(SiR_3)(PH_3)$_2$ and Pt(CH_3)(SiR_3)(PH_3)(C_2H_4) (R = Me or Cl), and the energy changes of Chalk−Harrod and modified Chalk−Harrod mechanisms of *cis*-PtH(SiR_3)(PH_3)$_2$ (R = Me and Cl) (12 pages). Ordering information is given on any current masthead page.

OM980190A